한국항해항만학회 제29권 제1호 춘계학술대회논문집 pp. 147~152, 2005. 4

Automatic Detection Approach of Ship using RADARSAT-1 Synthetic Aperture Radar

Chan-Su Yang, Seung-Joon Kwon**, In-Young Gong****

* *Senior Researcher, Maritime Safety and Pollution Control Research Division, KRISO/KORDI, Daejon, 305-600, Korea*
***School of Civil, Urban & Geo-Systems Engineering Seoul National University, Korea*
*** *Director, Maritime Safety and Pollution Control Research Division, KRISO/KORDI, Daejon, 305-600, Korea*

Abstract : *This paper proposes and evaluates a new approach to detect ships as targets from Radarsat-1 SAR (Synthetic Aperture Radar) imagery in the vicinity of Korean peninsula. To be more specific, a labeling technique and morphological filtering in conjunction with some other methods are employed to automatically detect the ships. From the test, the ships are revealed to be detected. For ground truth data, information from a radar system is used, which allows assessing accuracy of the approach. The results showed that the proposed approach has the high potential in automatically detecting the ships.*

Key words : *Radarsat-1, Otsu's method, morphological filter, ship detection*

1. Introduction

The ship monitoring systems that use the conventional ground-based radar system are constantly faced with difficulties during surveillance of moving ships due to the limited detection range. The space-based SAR(Synthetic Aperture Radar) images have shown to effectively monitor moving ships and stationary ships effectively[1),2),3),4)]. Unlike airborne and ground-based radars, space-based SAR is capable monitoring larger area compared with those of radars without the field of view limitations. In addition, this SAR sensor can also operate under any weather conditions and over a wide range.

There are two fundamentally different ways of detecting ships using the SAR images: detection of the ship target itself and detection of the ship wake. Some previous papers on this topic considered only either the ship wakes or ship target itself to perform the desirable detection, while there are other papers that considered both alternatives.

The work presented in this paper focuses on the procedure of detecting ship target itself in Radarsat-1 SAR imagery in a fully automatic way, because stationary ships and slow moving ships have no wakes and their wakes are often not visible in most cases. Ships are normally identified as very bright objects due to the corner reflection.

With the increasing importance in monitoring ship traffic in both coastal and ocean waters, an automatic detection of ships, wakes, and ship velocity is very desirable4). By using land-based radar, Vessel Traffic Service (VTS) has been developed and applied in waterways around ports. The control of ships near coasts is currently supported by VTS radar but it is restricted because of available information limitations. In addition to that, the coverage of monitoring ships by the traditional VTS is limited to the bay area or the approach from the sea to a harbour because of the radar range of about 10nm. There is a requirement for improving the VTS to be able to cover areas where radar coverage is almost impossible to achieve.

In this paper, the proposed method is to utilize the difference of pixels intensity between ships and sea clutter. The method to searching radar bright objects is

* Corresponding Author : Chan-Su Yang, yangcs@kriso.re.kr, 042)868-7276
** Seung-Joon Kwon, kwonsj77@snu.ac.kr
*** In-Young Gong, iygong@kriso.re.kr, 042)868-7261

to fix a global image threshold and then set a pixel intensity above this threshold as the target of interest.

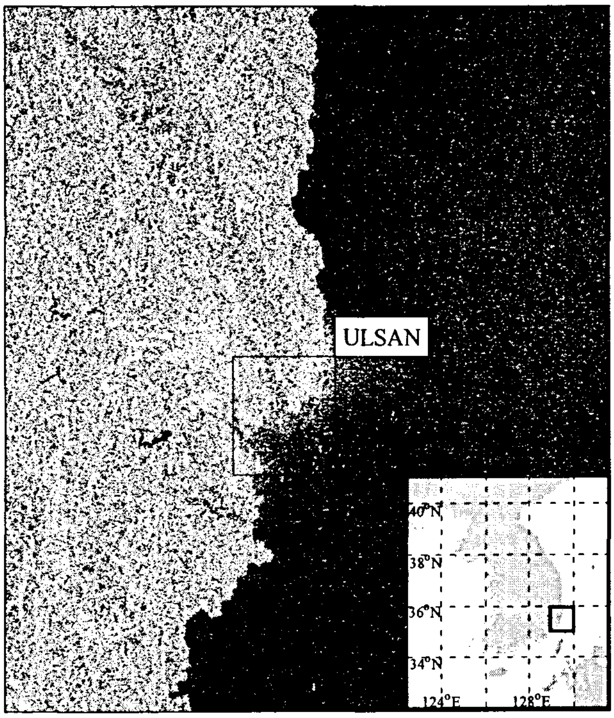

Fig. 1 RADARSAT image, Ulsan Bay- centered East Coast of South Korea, June 19, 2004.

In this study, a fixed threshold using Otsu's method and k-distribution was applied and the main processes involve combining the labeling technique and morphological filtering in order to detect ships automatically.

2. Data

2.1 SAR Image Data: Fine Mode

The SAR aboard RADARSAT-1 operates in the C-band and with horizontal transmit and horizontal receive polarization (C-HH). SAR images cover a swath width of about 45 km and have an across-track spatial resolution of about 9m. This instrument can produce images in seven different modes and with multiple viewing angles ranging from 10° to 59°. RADARSAT-1 is sun-synchronous satellite operating in near polar orbit at altitudes of about 800 km. In the case of ship detection, the probability of detection is enhanced at large incidence angles.

RADARSAT-1 satellite SAR data acquired on June 19, 2004 and processed at the Korea Earth Observation Center (KEOC) as shown in Fig. 1. The Fine mode is processed to the path image plus level (SGX) with 3.125m pixel spacing (F2) and the incidence angle is 41.2°. SAR image is calibrated to geophysical (sigma naught) values of radar cross section (RCS) even if data numbers (DN) on these detected images can be viewed as indicating relative radar backscatter intensities.

2.2 Wind and Ship Information: VTS

Wind and radar data were acquired at Hwaamchu site and transmitted to VTS center (PTMS in Fig. 2). The line in Fig. 2 shows a trajectory moved aboard a pilot ship. VTS refers to the services promoting effectiveness improvement in port operation and reduction in distribution cost by providing counsel or required information for safe vessel service within the range of not violating rights or exempting obligations of the shipmaster via observing movement of vessels in port area and entrance routes with the latest scientific devices of radar, CCTV and VHF, etc. for the purpose of increasing vessel safety and effectiveness as well as of protecting environment.

During the field experiment, northwest winds, with speeds from 2.6 m/s to 3.2 m/s were recorded with 0.5 m significant wave height. VTS tracks most shipping traffic using shore-based radar. VTS data are available at twelve-second intervals and consist of a vessel code (ship name, position, speed, course and speed) on a map. The code can be used to ascertain ship length, breadth, depth, and type, and the VTS display can be overlaid with radar images of ships.

A pilot ship was going around at Ulsan anchorage under the RADARSAT pass and boarded taking photos of ships along the line as shown in Fig. 2.

3. Ship Detection using RADARSAT-1 Synthetic Aperture Radar

3.1 Otsu's method

The purpose of this method is to automatically divide an image's light intensity histogram into two distinct regions while performing unsupervised, that is, without requiring a human to supply any threshold information. Optimal thresholds are critical for extracting foreground objects when a statistical histogram approach is employed. There is a method which is applied gray-level images. A discriminant analysis is performed

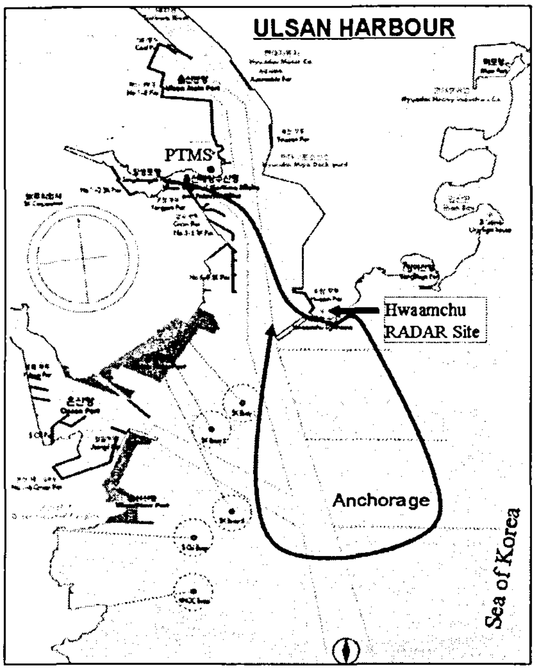

Fig. 2 Map of Ulsan Bay. Radar and weather data were measured at Hwaamchu site. The bold line represents a trajectory of ship used here.

to divide the foreground and background by maximizing the discriminant measure variable. An image is a 2D grayscale intensity function, and contains N pixels with gray levels ranging from 1 to L. The number of pixels with gray level i is denoted as n, giving a probability of gray level i in an image of $p_i=n_i/N$.

In the case of applying bi-level thresholding for an image, the pixels are broken into two classes, C1 with gray levels [1, ..,t] and C2 with gray levels [t+1,⋯,L]. Then, the gray level probability distributions for the two classes are

C1: $P1/\omega_1(t),...p_t/\omega_1(t)$ and

C2: $Pt+1/\omega_2(t)$, $Pt+2/\omega_2(t),\cdots,P_L/\omega_2(t)$,

where $\omega_1(t)=\sum_{i=1}^{t}P_i$ and $\omega_2(t)=\sum_{i=t+1}^{L}P_i$.

The mean intensities of the classes C1 and C2 can be obtained using

$$\mu_1=\sum_{i=1}^{t}iP_i/\omega_1(t) \quad (1)$$

$$\mu_2=\sum_{i=t+1}^{L}iP_i/\omega_2(t) \quad (2)$$

Assuming that μ_T is the mean intensity for the entire image. Thus

$$\omega_1\mu_1+\omega_2\mu_2=\mu_T,\omega_1+\omega_2=1 \quad (3)$$

Through the discriminant analysis, Otsu defined the interclass variance of the thresholded image.

$$\sigma_B{}^2=\omega_1(\mu_1-\mu_T)^2+\varpi_2(\mu_2-\mu_T)^2 \quad (4)$$

For bi-level thresholding, Otsu verified that the optimal threshold t* is chosen so that interclass variance $\sigma_B{}^2$ is maximized. So t*= Arg Max{$\sigma_B{}^2(t)$} ($1\le t<L$).

The problem reduces to a simple search for the optimal t value, namely, the t value that produces the largest $\sigma_B^2(t)$. However the previous formula can be extended to multilevel thresholding of an image. Assuming that there are M-1 thresholds, {t1 ,t2 , ..,t $_{M-1}$}, which divide the original image into M classes: C1 for [1,⋯, t1], C2 for [t1+1,⋯, t2],⋯,Ci for [ti-1+1 ,⋯,ti],⋯,and CM for [tM-1+1,⋯,L], the optimal thresholds { t1* ,t2*,⋯, tM-1*} are chosen by maximizing $\sigma_B{}^2$ as follows:

$$\{t_1*,t_2*,\cdots,t_{M-1}*\}=\text{Arg Max}\{\sigma_B{}^2(t_1,t_2,..,t_{M-1})\}$$

$$1\le t_1<...<t_{M-1}<L$$

where $\sigma_B{}^2=\sum_{k=1}^{M}\omega_k(\mu_k-\mu_T)^2$ with

$$\omega_k=\sum_{i\in C_K}p_i, \quad (5)$$

$$\mu_k=\sum_{i\in C_K}ip_i/\omega(k) \quad (6)$$

The ω_K in Eq. (5) is discovered as the Zeroth order cumulative momentof the Kth class C_K, and the numerator in Equ. (6) is discovered as the first order

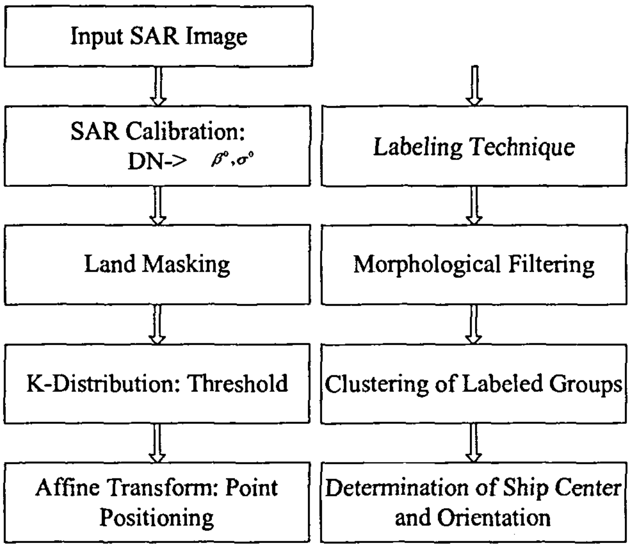

Fig. 3 Flowchart of the proposed algorithm

cumulative moment of the Kth class C_K that is to say

$$\mu(k) = \sum_{i \in C_K} iP_i \tag{7}$$

3.2 Ship Detection Algorithm

The proposed structure of the detection algorithm is *illustrated in Figure 3. The process flow of the* proposed algorithm is as follows: After utilizing the Otsu's method for optimal image thresholding, we convert the input image to grayscale format, and then convert this grayscale image to binary by thresholding. The output binary image has values of 0 (black) for all pixels in the input image with luminance less than level and 1 (white) for all other pixels(because we specify level in the range [0,1], regardless of the class of the input image). Next we label connected components specifying 8-connected objects in the binary image(Fig. 4). The pixels labeled 0 are the background. The pixels labeled 1 make up one object, the pixels labeled 2 make up a second object, and so on.

$$\begin{matrix} 1 & 1 & 1 & 0 & 0 & 0 & 0 & 0 \\ 1 & 1 & 1 & 0 & 1 & 1 & 0 & 0 \\ 1 & 1 & 1 & 0 & 1 & 1 & 0 & 0 \\ 1 & 1 & 1 & 0 & 0 & 0 & 0 & 0 \\ 1 & 1 & 1 & 0 & 0 & 0 & 1 & 0 \\ 1 & 1 & 1 & 0 & 0 & 0 & 1 & 0 \\ 1 & 1 & 1 & 0 & 0 & 0 & 0 & 0 \end{matrix} \quad \Rightarrow \quad \begin{matrix} 1 & 1 & 1 & 0 & 0 & 0 & 0 & 0 \\ 1 & 1 & 1 & 0 & 2 & 2 & 0 & 0 \\ 1 & 1 & 1 & 0 & 2 & 2 & 0 & 0 \\ 1 & 1 & 1 & 0 & 0 & 0 & 0 & 0 \\ 1 & 1 & 1 & 0 & 0 & 0 & 3 & 0 \\ 1 & 1 & 1 & 0 & 0 & 0 & 3 & 0 \\ 1 & 1 & 1 & 0 & 0 & 0 & 0 & 0 \end{matrix}$$

Fig. 4 This illustrates using 8 connected objects. 8-connected labeling perceives these a single object rather than two separate objects.

Next, we find the labeled groups which have more than 10 pixels size, because we also focus on the detection of the relatively large ships such as bulk carrier, container ship, etc. The pixel size threshold in this work is varied with the pixel dimension of SAR image.

A morphological filtering is performed to reduce suspicious noise still remaining in the previous step. The combination of the dilation and erosion of morphological filtering is processed to enhance the boundary of the identified ship candidates more clearly. The dilation operation fills the black pixels inside a ship pixel cluster. It also connects neighboring ship candidate pixels. While dilation adds pixels to the boundaries of objects in an image, erosion removes pixels on object boundaries. The erosion operation also weakens geometric distortion after dilation operation. After the ship candidates are identified approximately, clustering with respect to the distance between central values of the individual pixel groups labeled in the previous work is processed in the whole image to weaken the probability of misidentification of labeled groups using optimal scale factor. However there is still a possibility of misidentifying labeled groups due to unexpected speckle noise. Thus, it is necessary calculate the minimum of distance between all pixels that belong to the Nth labeled pixel group and all pixels that belong to (N+1)th labeled group. This minimum distance value can refine and re-label pixel groups (ship candidate) which in turn could reduce the likelihood of misidentifying in a fast way. Lastly, accuracy evaluation by comparison with ground truth data from the coast monitoring system should follow.

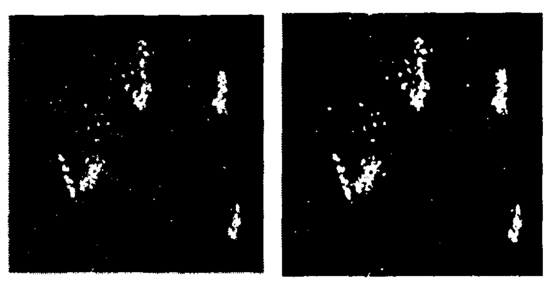

Fig. 5. original sample image(left), threshed binary image using Otsu's method(right)

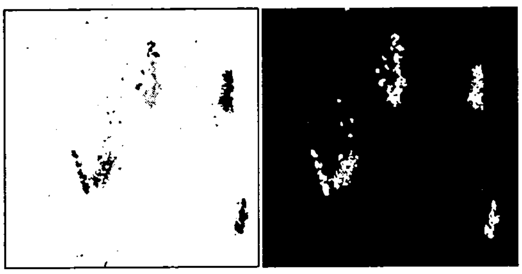

Fig. 6. labeled image to RGB color(left), labeled ID>10 pixel(scale factor)(right)

Table 2 labeled group ID & pixel numbers

ID	1	2	3	4	5	6	7	8	9	10	11	12	13	14	15	16	17	18	19	20
Pixel #	1	4	1	1	1	3	3	2	2	4	2	1	4	4	2	7	44	1	2	54
ID	21	22	23	24	25	26	27	28	29	30	31	32	33	34	35	36	37	38	39	40
Pixel #	16	1	1	1	1	5	45	4	3	1	2	2	2	11	25	1	1	11	1	1
ID	41	42	43	44	45	46	47	48	49	50	51	52	53	54	55	56	57	58	59	60
Pixel #	2	5	14	2	9	6	4	2	1	6	13	4	1	12	12	1	3	3	6	3
ID	61	62	63	64	65	66	67	68	69	70	71	72	73	74	75	76	77	78	79	80
Pixel #	2	6	3	8	8	3	3	6	1	1	2	4	3	2	2	16	38	2	4	13
ID	81	82	83	84	85	86	87	88	89	90	91	92	93	94	95	96	97	98	99	10
Pixel #	15	1	49	2	8	74	2	7	2	40	2	1	1	3	1	1	1	7	3	3
ID	10	10	10	10	10	10	10	10	10	11	11	11	11	11	11	11	11	11	11	12
Pixel #	1	3	1	2	5	4	1	1	2	4	4	2	50	2	5	4	1	2	1	27
ID	12	12	12	12	12	12														
Pixel #	2	3	7	1	1	1														

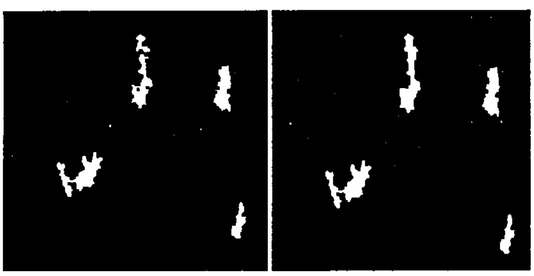

Fig. 7. labeled image using morphologic filter(left), clustering centroid of label groups& refining(right)

Fig. 8. centroids of label group

3.3 Dtection Results

We applied the method for a Radarsat-1 sample image (300 by 270, Fig. 5.) in order to evaluate its performance. Like other prescreening algorithms, not all pixels detected by this process will be true ship pixels and further processing is required to remove such false pixels.We obtained regional properties oflabel group(ship candidate) such as centroids(x,y), area, minor axis length, etc., from the previous step. After evaluating the accuracy of the position with these centroids, HACE(see Figure 9.) could be interpreted as the detected ship in the sample image. Basically, we were able to confirm that the position of the ship candidates in the sample region agreed with the position reported in the Ulsan coast monitoring system.

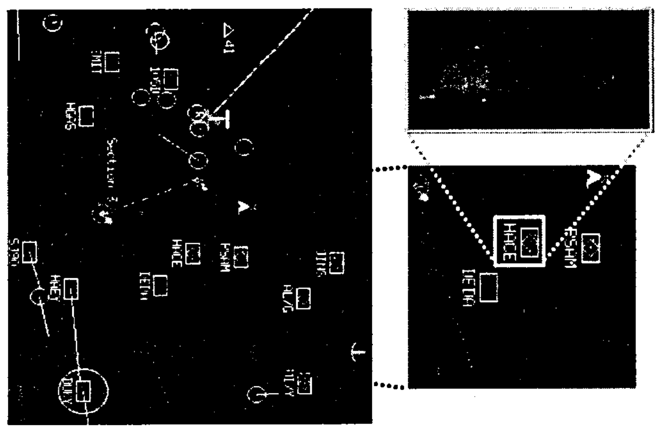

Fig. 9. Ground truth for sample region (left, right bottom), HACE ship (right top)

6. Concluding Remarks

In this paper, we introduced a ship detection technique by applying the labeling technique, morphological filtering, and Otsu's method. The main advantage of the method is that the difference of light intensities between a ship and the sea can be obtained quickly and automatically without human intervention. A disadvantage, however, is that not all pixels detected by this method will be true ship pixels, requiring further processing to be conducted to remove such false pixels. In the future, we plan to conduct studies on improving this method and test it on a large scale sample to verify its effectiveness.

Acknowledgement

This work was supported by the Basic Research Project, "Development of Basic Technology of Total

Risk Management for Marine Systems" and "Development of Safety Evaluation Technologies for Marine Structures in Disastrous Ocean Waves", and the Public Benefit Project of Remote Sensing, "Risk Map of Marine Accidents Based on Satellite Data" of Korea Aerospace Research Institute and the national specific research and development project, "Development of Marine Traffic Safety Information System and Oil Spill Monitoring System based on Artificial Satellite" of the Ministry of Science & Technology.

References

[1] Yang, C.S. and Park, Y.S., Merging of satellite remote sensing and environmental stress model for ensuring marine safety. Intl. J. Navigation and Port Research, 27(6), pp. 645-652, 2003.

[2] Morse, A.J. and Protheroe, M.A., Vessel classification as part of an automated vessel traffic monitoring system using SAR data. Intl. J. Rem. Sensing, 18(13), pp. 2709-2712,1997.

[3] Vachon, P., Campbell, J., Bjerkelund, C., Dobson, F., and Rey, M., Validation of Ship detection by the RADARSAT SAR, Proceedings PORSEC'96, Victoria, Canada, 1996.

[4] Vachon, P.W., Campbell, J., Bjerkelund, C., Dobson, F., and Rey, M., Ship Detection by the RADARSAT SAR: Validation of Detection Model Predictions, Canadian Journal of Remote Sensing, 23(1), pp. 48-59, 1997.

[5] ElDhuset, K., An automated ship and ship wake detection system for spaceborne SAR images in coastal regions, IEEE Trans. Geosci. Remote Sensing, vol. 34, no. 4, pp.553-560,1996.

[6] Otsu, N., A threshold selection method from graylevel histogram, IEEE Trans. System Man Cybernetics, vol. SMC-9, no.1, pp. 62-66, 1979.